Supplementary Information:

Oxygen Ion Transport in Doped Ceria:

Effect of Vacancy Trapping

Mehmet Emin Kilic[a], Jong-Ho Lee[b], Kwang-Ryeol Lee[a,*]

[a]Computational Science Center, Korea Institute of Science and Technology, Seoul, Republic of Korea

[b]Center for Energy Materials Research, Korea Institute of Science and Technology, Seoul, Republic of Korea

Corresponding author: e-mail: krlee@kist.re.kr

Structure Relaxation

Ionic diffusion analysis is performed using the thermally relaxed structures. To obtain the thermally equilibrated systems, all structures are first exposed to total energy minimization and then the quenching and annealing processes. First, each initial configuration (unrelaxed) has been optimized by the conjugate gradient energy minimization, which relaxes the position of ions to a lower energy configuration. After the energy minimization process, the quenching and annealing processes are set to accelerate the equilibration process for each system under a temperature gradient. This approach directs the positions of vacancies and ions to the global minimum in avoidance of artificial defect formation. The thermal equilibration process is performed as follows: The system is first heated to 2000 K using a constant pressure and temperature ensemble (NPT) to ensure thermal equilibrium is reached for the desired temperature. Thereafter,

the constant volume and energy ensemble (NVE) is enforced, and the NVE MD simulation runs for 500 ps. Subsequently, the system is then rapidly cooled down (hence, quenched) from 2000 to 300 K with the NPT ensemble for 50 ps and then further relaxed for another 200 ps with the NVE ensemble. Finally, the system is equilibrated with NPT and NVE ensembles at 300 K temperature. With this thermally equilibration process, the thermally relaxed atomic structures for a given target temperature are then used for further analysis.

Computational Details

In the static LD calculations, the ion polarizability was considered for Ce^{4+} and O^{2-} through the shell model [1]. The parameters and details are given in the Reference 2. However, the doped ions were assumed to be unpolarizable due to the lack of the available potential. It was reported that the polarization of the dopant in doped ceria has little influence on the results [2-4]. For MD simulations, a rigid ion model was used as in other publications [5-7]. Using the Grimes potential in the rigid-ion approximation, the predicted oxygen migration energy was in excellent agreement with the experimental results [8].

We compared the calculated lattice parameters of CeO_2 and 10GDC with those of DFT calculation or experimentally reported values as shown in Table S1. According to the DFT calculations, the lattice constant of CeO_2 is found to be 5.50 Å, agreeing well with the previous theoretical values, 5.49 [9,10]. The DFT results tend to show a larger value for the lattice parameters than experiments due to the underestimation of the bond strength by employing semi-local exchange correlation functions. On the other hand, lattice dynamics (LD) results reproduce the lattice parameters of CeO_2 and GDC in experimental values.

Table S1 Calculated lattice constants *a* of CeO_2 and GDC by employing DFT (at PBE+U level) and lattice dynamics (LD) calculations.

	CeO_2 ***a* (Å)**	**GDC** ***a* (Å)**
DFT	5.50	5.51
LD	5.42	5.43
Experiments	5.42[a]	5.42[b]

[a] Ref. 11 and [b] Ref.12.

References:

[1] *Phys. Rev.* **112**, 90, (1958); [2] *Solid State Ion.* **116**, 339 (1999); [3] *Solid State Ion.* **180**, 13 (2009); [4] *Chem. Mater.* **15**, 3781 (2003); [5] Nat. Commun. **6**, 1 (2015); [6] *Phys. Chem. Chem. Phys.* **21**, 980 (2019); [7] *Acta Mater*. **210**, 116802 (2021); [8] *Solid State Ion.* **181**, 551 (2010); [9] *J. Mater. Chem. A,* **2**, 13723 (2014); [10] *Phys. Rev.* **B75**, 045121 (2007); [11] *J. Alloys Compd.* **400**, 56 (2005); [12] *J. Alloys Compd.* **115**, 44 (2003).

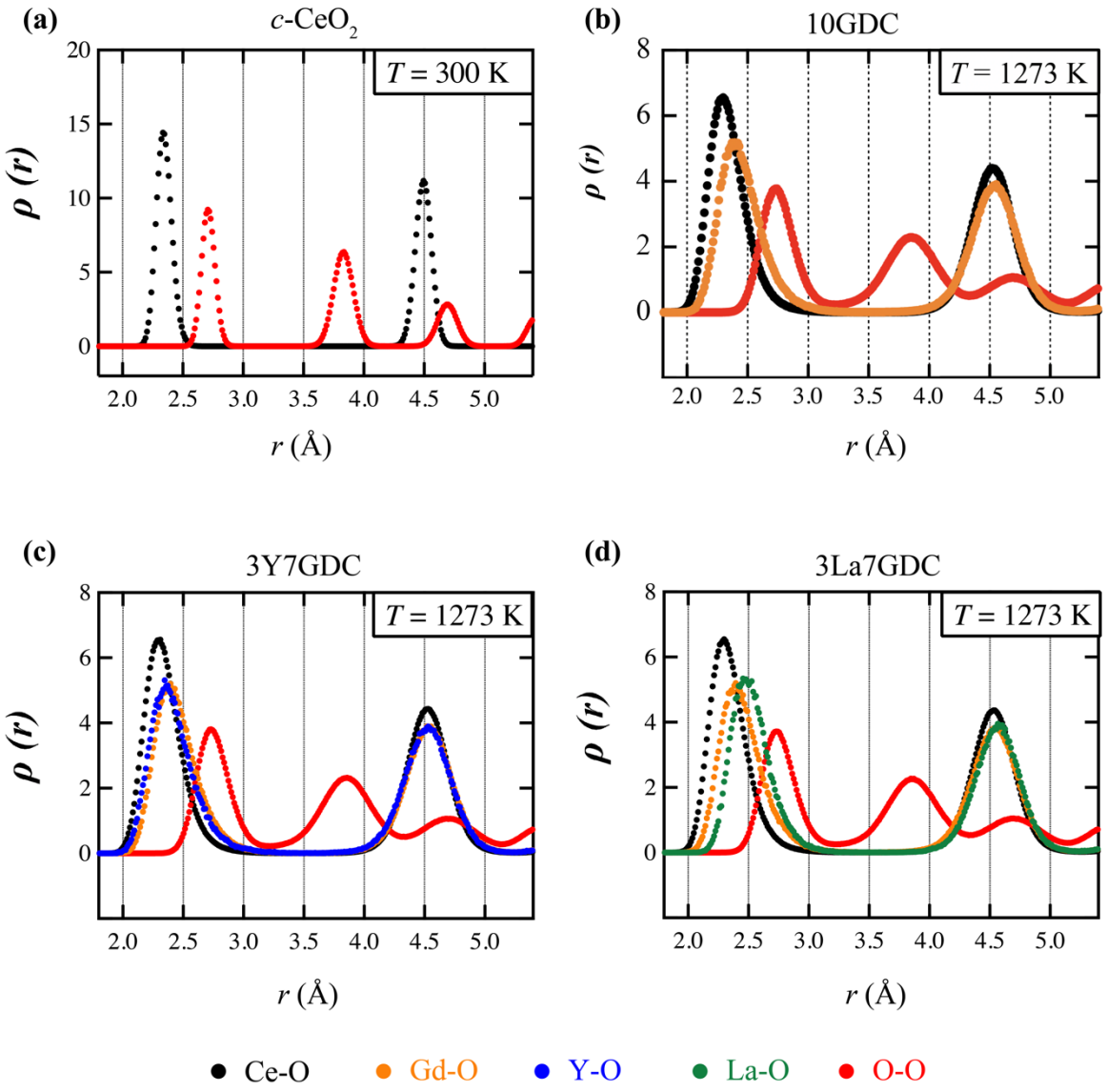

Fig. S1 Calculated radial distribution functions (RDF) of (a) cubic CeO_2 at 300 K, (b) 10GDC, (c) 3Y7GDC, and (d) 3La7GDC at 1273 K temperature. Here, the black, yellow, blue, green, and red markers represent the RDF between Ce^{4+}–O^{2-}, Gd^{3+}– O^{2-}, Y^{3+}– O^{2-}, La^{3+}– O^{2-}, and O^{2-} – O^{2-}.

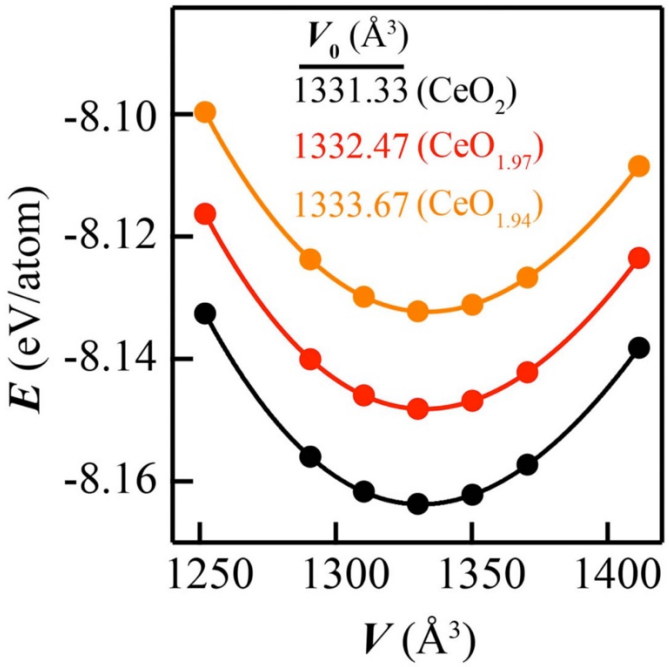

Fig. S2 The energy (in eV/atom) - volume (in Å^3) curves of CeO_x (x = 2, 1.97, and 1.94). The markers represent the DFT total energies and the solid lines are fitted to the 3rd order Birch-Murnaghan equation-of-state.

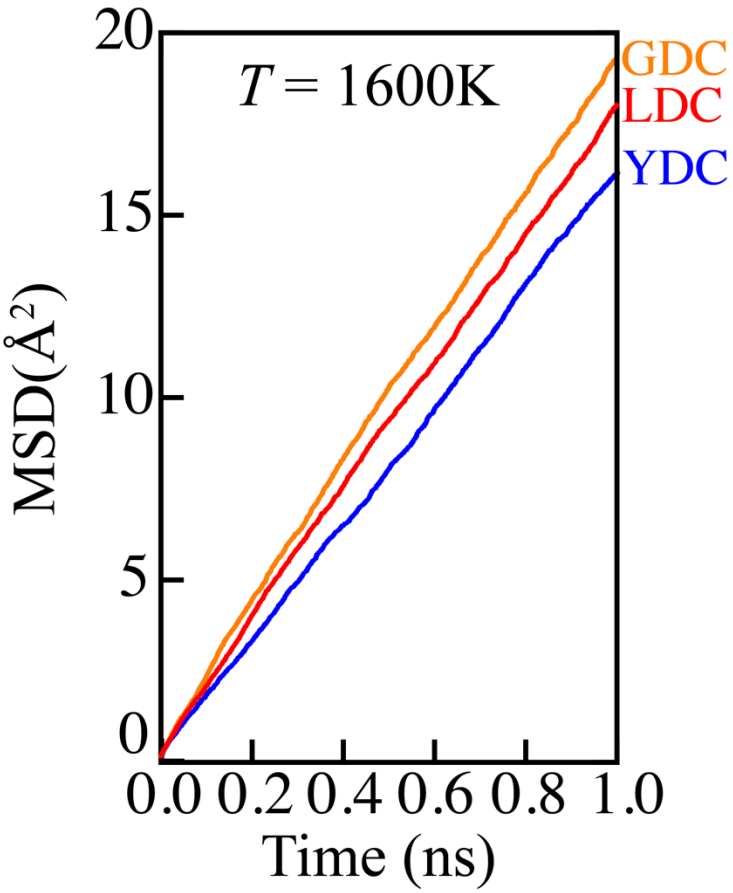

Fig. S3 Mean square displacements in $Å^2$ for oxygen ions for 10GDC, 10YDC, and 10LDC (in orange, blue, and red lines, respectively) at $T = 1600$ K for 1 ns.

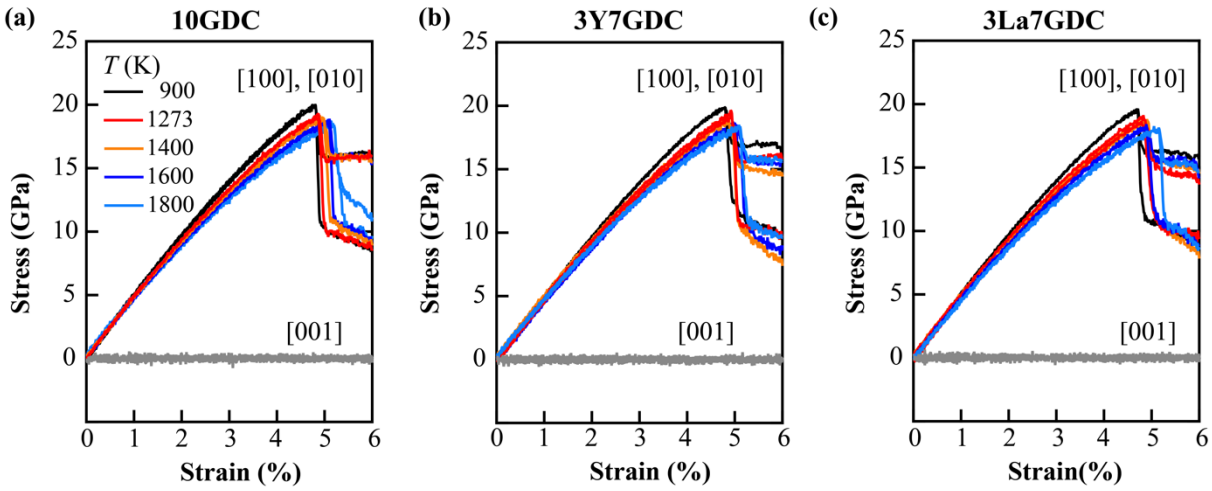

Fig. S4 Variation of stress along the [100], [010], and [001] lattice directions with respect to applied equi-biaxial tensile strain along the [100] and [010] plane for 10GDC, 3Y7GDC, and 3La7GDC at the range of temperatures from 900 to 1800 K. Here, the systems along the [001] direction are optimized with NPT ensemble which allows atm pressure while optimized with NVT ensemble along the [100] and [010] directions.